Applied Physics Letters

RESEARCH ARTICLE | JULY 17 2023

Detecting driving potentials at the buried SiO_2 nanolayers in solar cells by chemical-selective nonlinear x-ray spectroscopy

Masafumi Horio ; Toshihide Sumi ; James Bullock ; Yasuyuki Hirata; Masashige Miyamoto ; Bailey R. Nebgen ; Tetsuya Wada; Tomoaki Senoo ; Yuki Tsujikawa ; Yuya Kubota ; Shigeki Owada ; Kensuke Tono ; Makina Yabashi ; Takushi Iimori; Yoshihiro Miyauchi; Michael W. Zuerch ; Iwao Matsuda ; Craig P. Schwartz ; Walter S. Drisdell

Appl. Phys. Lett. 123, 031602 (2023)
https://doi.org/10.1063/5.0156171

AIP Publishing

Applied Physics Letters ARTICLE pubs.aip.org/aip/apl

Detecting driving potentials at the buried SiO_2 nanolayers in solar cells by chemical-selective nonlinear x-ray spectroscopy

Cite as: Appl. Phys. Lett. **123**, 031602 (2023); doi: 10.1063/5.0156171
Submitted: 27 April 2023 · Accepted: 29 June 2023 ·
Published Online: 17 July 2023

Masafumi Horio,[1,a] Toshihide Sumi,[1] James Bullock,[2] Yasuyuki Hirata,[3] Masashige Miyamoto,[1] Bailey R. Nebgen,[4,5] Tetsuya Wada,[1] Tomoaki Senoo,[1] Yuki Tsujikawa,[1] Yuya Kubota,[6] Shigeki Owada,[6,7] Kensuke Tono,[6,7] Makina Yabashi,[6,7] Takushi Iimori,[1,8] Yoshihiro Miyauchi,[3] Michael W. Zuerch,[4,5] Iwao Matsuda,[1,8] Craig P. Schwartz,[9] and Walter S. Drisdell[10,11]

AFFILIATIONS

[1]Institute for Solid State Physics, The University of Tokyo, Kashiwa, Chiba 277-8581, Japan
[2]Electrical and Electronic Engineering, The University of Melbourne, Victoria 3010, Australia
[3]National Defense Academy of Japan, Yokosuka, Kanagawa 239-8686, Japan
[4]Department of Chemistry, University of California, Berkeley, California 94720, USA
[5]Materials Sciences Division, Lawrence Berkeley National Laboratory, Berkeley, California 94720, USA
[6]RIKEN SPring-8 Center, 1-1-1 Kouto, Sayo, Hyogo 679-5148, Japan
[7]Japan Synchrotron Radiation Research Institute (JASRI), 1-1-1 Kouto, Sayo, Hyogo 679-5198, Japan
[8]Trans-scale Quantum Science Institute, the University of Tokyo, Hongo, Bunkyo-ku, Tokyo 113-8654, Japan
[9]Nevada Extreme Conditions Laboratory, University of Nevada, Las Vegas, Las Vegas, Nevada 89154, USA
[10]Chemical Sciences Division, Lawrence Berkeley National Laboratory, Berkeley, California 94720, USA
[11]Liquid Sunlight Alliance, Lawrence Berkeley National Laboratory, Berkeley, California 94720, USA

[a]**Author to whom correspondence should be addressed:** mhorio@issp.u-tokyo.ac.jp

ABSTRACT

We present an approach to selectively examine an asymmetric potential in the buried layer of solar cell devices by means of nonlinear x-ray spectroscopy. Detecting second harmonic generation signals while resonant to the SiO_2 core level, we directly observe existence of the band bending effect in the SiO_2 nanolayer, buried in the heterostructures of Al/LiF/SiO_2/Si, TiO_2/SiO_2/Si, and Al_2O_3/SiO_2/Si. The results demonstrate high sensitivity of the method to the asymmetric potential that determines performance of functional materials for photovoltaics or other optoelectronic devices.

The photovoltaics industry is currently dominated by solar cells based on crystalline silicon. Technical development of these cells focuses on increasing the power conversion efficiency and reducing the production costs.[1] Recent years have seen the development of new "passivated contact" or "carrier-selective contact" architectures which, instead of relying on a traditional diffused p–n junction, utilize specialized contact interfaces to separate out electrons and holes.[1–7] These interfaces are commonly composed of stacks of thin films, which collectively passivate the crystalline silicon surface and provide a strong asymmetry in conductivity to electrons and holes.[5–7] As such, there is a growing emphasis on controlling the properties of these thin films and contact interfaces in silicon photovoltaics. To further develop these systems, direct observation of the microscopic states in the composing layer or interface is needed, since these states dictate the macroscopic performance. However, selectively examining electronic states at the buried region of a complex heterostructure is spectroscopically challenging with conventional electronic analysis techniques such as x-ray photoelectron spectroscopy (XPS) or x-ray absorption spectroscopy (XAS). These techniques probe either the bulk of the material or its top surface with no way to selectively probe a buried interface. The electronic structure of these systems has, therefore, been deduced from an array of indirect spectroscopic probes.

In the present research, we used an efficient experimental approach to selectively probe electronic states in the functional layer of a solar cell by means of nonlinear x-ray spectroscopy, specifically core-level-resonant x-ray second harmonic generation (x-ray SHG), using an x-ray free-electron laser source.[8] The development of this method was motivated by the fact that the photovoltaic effect is induced by electron–hole separation due to an asymmetric potential in the heterostructure. Since the SHG signal is only generated from regions that lack inversion symmetry, it should specifically probe the interface between the components of the heterostructure. This sensitivity, combined with the selectivity for specific elements and electronic states that x rays afford, allows us to detect the driving potential at the buried layer in a solar cell. Measurements of core-level-resonances using x-ray SHG have been successfully made with x-ray free-electron lasers in the soft x-ray region.[9–15] Recently, the achievements have extended to lithium-containing materials relevant to battery applications.[11,12,15]

Figure 1(a) shows a schematic drawing of the x-ray SHG experiment, conducted at the soft x-ray free-electron laser (SXFEL) beamline BL1 of SACLA.[16,17] The beamline covers the photon energy range of $\hbar\omega = 26$–150 eV with an XFEL pulse of <10 fs-width, 80 μJ, and energy resolution of $\Delta E/E = \Delta(\hbar\omega)/\hbar\omega \sim 2\%$. The incident beam ($\hbar\omega$) was focused to 5.3 μm (horizontal) $\times$ 1.0 μm (vertical) by a Wolter mirror and irradiated at the samples with an incident angle of 45° from the surface plane.[18,19] At this angle, specular reflectivity of the incident beam is on the order of 10^{-3} for all samples and on the order of 10^{-5} for any second harmonic photons from the FEL source (supplementary material Fig. S1). The SHG signal ($2\hbar\omega$) and the reflected beam ($\hbar\omega$) were monitored by an ellipsometry unit that separates the second order light from the beamline source[20–22] (see the supplementary material for more details about FEL measurements).

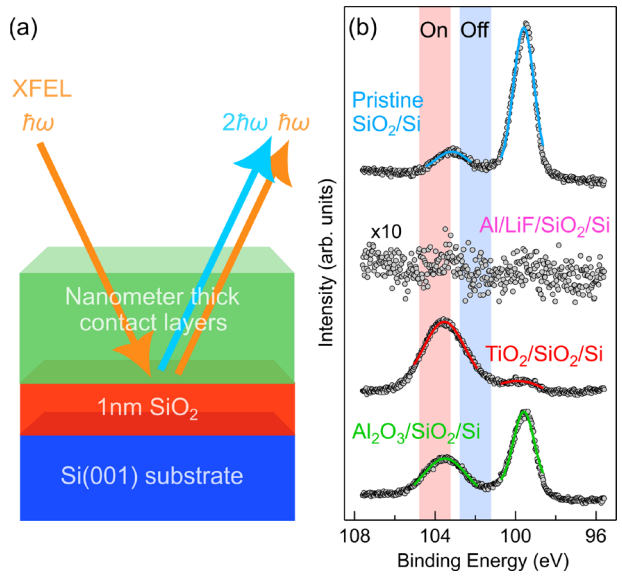

FIG. 1. Sample characterization. (a) Illustration of the x-ray SHG experiments on multilayer samples that contain 1 nm-thick SiO_2 layers, sandwiched between a Si substrate and a contacting layer. (b) X-ray photoelectron spectra of four samples with the curve-fitting results of the core-level peaks. The energy positions of the on-resonance and off resonance conditions for the XFEL beam are indicated by the red and blue shaded areas with a width of the energy resolution at the beamline, respectively.

The multilayered samples were composed of a Si(001) crystal substrate, a 1 nm-thick SiO_2 layer, and a nanometer-thick contacting layer. Measurements were made with three types of samples with different layers: Al/LiF/SiO_2/Si (LiF = 1 nm, Al = 5 nm), TiO_2/SiO_2/Si (TiO_2 = 2.5 nm), and Al_2O_3/SiO_2/Si (Al_2O_3 = 2.7 nm). The Al/LiF/SiO_2/Si system has been demonstrated to make an electron-selective contact with low contact resistivity.[5] The TiO_2/SiO_2/Si contact has been shown to be electron- or hole-selective, depending on the growth and electrode conditions.[1–3,6,7] The Al_2O_3/SiO_2/Si heterostructure has been typically used as a standard passivation layer for Si solar cells.[4] Details of the sample preparation are described elsewhere.[5–7] For a reference, the native SiO_2 layer on the Si substrate was adopted as a pristine SiO_2/Si sample that corresponds to a heterostructure of vacuum/SiO_2/Si during the measurement.

Figure 1(b) shows XPS spectra of the samples taken with a hemispherical electron analyzer (Scienta Omicron R3000) and a laboratory x-ray source using the Mg Kα emission line (see the supplementary material for more details about XPS measurements.). For individual spectra, two prominent peaks are observed at binding energy, E_B, near 99.55 and 103.5 eV that are assigned to the Si^0 atoms in the Si substrate and the Si^{4+} atoms in the SiO_2 layer, respectively. Differences in the peak intensity for different samples are due to the different thicknesses of the contact layers on the SiO_2/Si system. For example, the Al/LiF/SiO_2/Si sample has the thickest contact layer (6 nm total thickness), resulting in very low XPS signal from the SiO_2 layer underneath, whose peak position is difficult to assess. In contrast, the Si^0 peak is large for the SiO_2/Si sample since there is no contact layer, and the photoelectrons from the Si substrate are only blocked by the native SiO_2 layer. By curve-fitting the peaks with a Gaussian function, each E_B position of the sample, except for that of Al/LiF/SiO_2/Si, is determined as listed in Table I. The Si^0 positions are similar to each other for all samples, as expected since they share the same Si substrate and the same SiO_2/Si interface. The Si^{4+} positions, however, were found to depend on the samples. The heterostructure samples with the contact layers have deeper E_B values than that of the pristine SiO_2/Si sample. This implies that the solar cell heterostructures have distinct band structures compared to the pristine sample. The Si atoms in the SiO_2 layer are subject to a different electronic potential, possibly due to the band-bending effect.[23,24,27–31]

Focusing on the SiO_2 layer that exists in all the solar cell samples, Fig. 2 shows the power dependence of the SHG signal from the TiO_2/SiO_2/Si heterostructure, taken at two different incident photon energies. One can find the nonlinear signal is larger when the incident

TABLE I. XPS peak positions of the Si 2*p* core-levels of the samples. Values of the binding energy, E_B (eV), were referred from the Fermi level and were determined by peak-fits with the Gaussian functions in Fig. 1(b).

Samples	E_B (eV) at Si^0	E_B (eV) at Si^{4+}
pristine SiO_2/Si	99.55 ± 0.01	103.26 ± 0.05
Al/LiF/SiO_2/Si	...	...
TiO_2/SiO_2/Si	99.52 ± 0.09	103.63 ± 0.01
Al_2O_3/SiO_2/Si	99.54 ± 0.01	103.52 ± 0.02

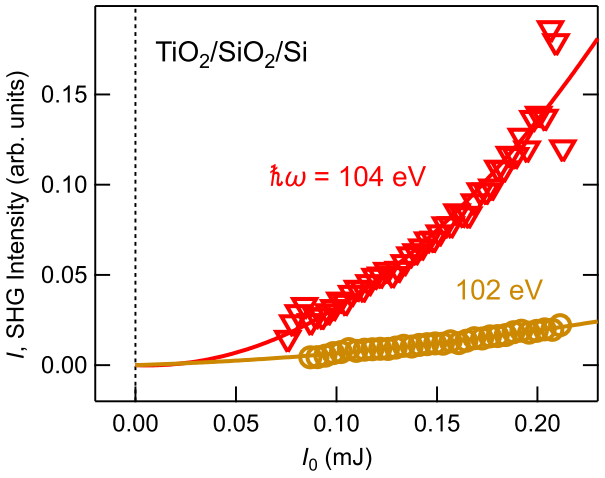

FIG. 2. Intensity of the SHG signal for the $TiO_2/SiO_2/Si$ sample with incident photon energies of $\hbar\omega = 104$ eV (on-resonance) and $\hbar\omega = 102$ eV (off resonance). The experimental data were fit by a polynominal curve, $I = aI_0 + bI_0^2$ with fitting coefficients, *a* and *b*. In the formula, *I* and I_0 are intensity of the measured and incident beams, respectively.

photons are on resonance with the Si^{4+} ($\hbar\omega = 104$ eV) vs off resonance ($\hbar\omega = 102$ eV) that are indicated in Fig. 1(b). This experimental observation indicates that the x-ray SHG is enhanced when the photon energy matches the core-level excitation energy of the chemical species at the atomic sites that lack local inversion symmetry.

Figure 3(a) collects x-ray SHG results for the four samples under the on-resonance condition, $\hbar\omega = 104$ eV. Individual datasets were fit by a polynominal with linear and nonlinear terms with respect to the incident power, I_0. The nonlinear or quadratic component corresponds to detection of SHG ($2\hbar\omega$), while the linear component corresponds to reflection of the fundamental beam ($\hbar\omega$). The contrast in the quadratic component between the samples [Fig. 3(b)] indicates the existence of SHG for the solar cell heterostructures, $Al/LiF/SiO_2/Si$, $TiO_2/SiO_2/Si$, and $Al_2O_3/SiO_2/Si$, but the absence of SHG for the pristine SiO_2/Si system. These optical responses mean that electronic states in the SiO_2 layer are subject to asymmetric potentials for the samples with contact layers and a symmetric potential for the pristine SiO_2/Si sample. This is likely due to differences in the band-bending effects at the junctions, consistent with the XPS results in Fig. 1(b).

In the case of the SiO_2/Si heterostructure, the symmetric characteristic indicates that the band in the thin SiO_2 layer is flat.[23,24] This is consistent with the wideband gap and sufficiently small amount of the space charges in this layer. Moreover, the magnitudes of the gap states at the SiO_2 surface and the SiO_2/Si interface have been reported to be $10^{11} - 10^{12}eV^{-1}cm^{-2}$, which are small enough to be negligible.[23] Thus, one can infer that the band-bending effect in the SiO_2 layer of the vacuum/SiO_2/Si heterostructure is too small to produce detectable SHG signals.

The existence of the asymmetric potential, yielding the SHG signal, is consistent with the functionality of the solar-cell heterostructures, $Al/LiF/SiO_2/Si$, $TiO_2/SiO_2/Si$, and $Al_2O_3/SiO_2/Si$. The appearance of the band-bending effect in the SiO_2 layer may be understood by employing the concepts of interfacial or surface gap states and charge neutrality level.[23] That is, differences between the chemical

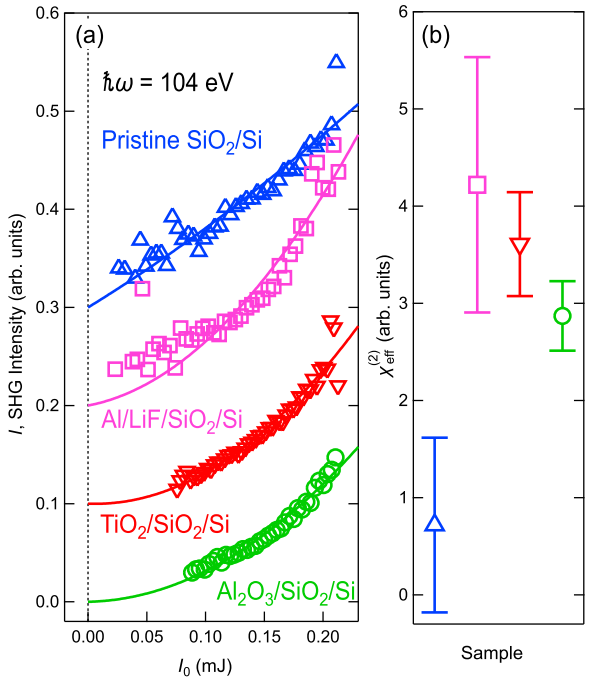

FIG. 3. Variation of the SHG signal from different samples. (a) Intensity curves of the samples, pristine SiO_2/Si, $Al/LiF/SiO_2/Si$, $TiO_2/SiO_2/Si$, and $Al_2O_3/SiO_2/Si$. Arbitrary vertical offsets are given for better visibility. The incident beam was set at a photon energy of $\hbar\omega = 104$ eV. The experimental data were curve-fitted by a polynominal, $I = aI_0 + bI_0^2$, as described in Fig. 2. (b) The value of $\chi^{(2)}_{eff}$ (coefficient *b*) for each sample. The error bar is based on the standard deviation of fitting.

potential of the contact layer and the SiO_2/Si layer become the driving force for charge transfer via gap states at the interface to electronically align the equilibrium chemical potential through the whole heterostructure. In that sense, particularly large band bending is expected between Al/LiF and SiO_2/Si due to the low work function Al/LiF electrode ($\phi \sim 2.9$ eV).[25,26] This is consistent with the observation of relatively large *b* value for $Al/LiF/SiO_2/Si$ [Fig. 3(b)], although, at present, large error bars prevent us from rigorously making a quantitative comparison with the *b* values from the other samples. In the asymmetric electronic potential of the studied SiO_2/Si systems with contact layers, bands in the SiO_2 layer are expected—from the XPS results [Fig. 1(b)] and previous studies[5]—to bend downward toward the contacting layer. This electronic structure serves to accept electrons transported from the Si substrate while blocking hole transport, creating an electron-selective contact, as expected. The SHG measurements reveal that the buried SiO_2 nanolayer is multi-functional, simultaneously passivating the Si interface, forming a stable contact, and hosting a carrier-driving asymmetric potential created by the deposition of contact layers.

It is worth discussing the differences between conventional measurements and the present SHG method to examine the degree of band-bending in each sample. Directly probed surface photovoltage measurements are often used to investigate band-bending, but this probes a bulk property of the entire device stack, whereas x-ray SHG is element-selective and, therefore, specifically probes an individual layer within the stack. Standard x-ray absorption measurements are also

element-selective, but typically bulk sensitive and, therefore, unable to detect thin layers such as SiO_2 in the samples studied here (supplementary material Fig. S2). XPS analysis combines element-selectivity and surface sensitivity, and when performed with a tunable x-ray source (such as a synchrotron light source) can determine depth profiles of the band energy by changing the probing depth of photoelectrons. More advanced time-resolved XPS measurements can also trace the carrier dynamics by the surface photovoltage effect. However, XPS experiments typically only probe a few nm of the sample surface.[27–31] For detecting photoelectrons, the signal is significantly attenuated for a buried layer of the heterostructure, as shown in Fig. 1(b). Moreover, a depth profiling measurement is required to capture the shape of the potential responsible for the band bending effect. In contrast, as shown in Fig. 3, x-ray SHG directly probes the asymmetric potential in the buried layer that is responsible for the functionalities of the heterostructure devices.

The x-ray nonlinear spectroscopy measurements reported here are conducted with a photon-in and photon-out configuration. Thus, variations in the asymmetric potential could be monitored in real time under working conditions, applied current, or applied voltage. Moreover, since the incident photon pulses are ultrafast, time-resolved measurements of x-ray SHG could be performed, providing the time constants that characterize the carrier dynamics. These *operando* experiments could reveal weak points at the junctions in devices and guide advanced designs that maximize the actual performance. X-ray SHG spectra could also be collected by scanning the input x-ray energy. Changes in the spectral shape would imply subtle differences in the interfacial electronic structure, as specific electronic states are probed at the interface, and properties, such as exact oxidation number, could be determined. The present research proves usefulness of the method for studying functional optical devices such as solar cells.

In summary, we presented an efficient approach to directly probe asymmetric electronic states in a selected layer that is responsible for the photovoltaic functionality of a heterostructure device. By irradiating XFEL pulses at the solar cell samples, the SHG signal from the buried layers was observed with enhancement of the signal under the core-level resonance condition. The results demonstrate high sensitivity to the asymmetric potential, which proves the usefulness of the technique for developing devices.

See the supplementary material for details of sample preparation, x-ray SHG, XPS, and reflectivity measurements.

The development was performed at the facilities of the Synchrotron Radiation Research Organization in the University of Tokyo. The XFEL experiments were performed at SACLA with the approval of the Japan Synchrotron Radiation Research Institute (JASRI) (Proposal No. 2022A8056). X-ray reflectivity measurements were performed at beamline 6.3.2 at the Advanced Light Source, which is a DOE Office of Science User Facility under Contract No. DE-AC02-05CH11231. T.S. acknowledges support by the Forefront Physics and Mathematics (FoPM) WINGS Program, the University of Tokyo. J.B. acknowledges support from the Australian Center for Advanced Photovolatics and Melbourne Center for Nanofabriaction Fellowship Programs. B.R.N. acknowledges funding by the National Science Foundation Graduate Research Fellowship Program. M.W.Z. acknowledges funding by the W. M. Keck Foundation, funding from the Hellman Fellows Fund, funding from the UC Office of the President within the Multicampus Research Programs and Initiatives (Nos. M21PL3263 and M23PR5931), funding from Laboratory Directed Research and Development Program at Berkeley Lab (Nos. 107573 and 108232), and the National Science Foundation (No. DMR-2247363). C.P.S. acknowledges the U.S. Department of Energy, Office of Science, Office of Basic Energy Sciences EPSCoR under Award No. DE-SC-0023397. W.S.D. acknowledges support from the Liquid Sunlight Alliance, which is supported by the U.S. Department of Energy, Office of Science, Basic Energy Sciences under Award No. DE-SC0021266.

AUTHOR DECLARATIONS

Conflict of Interest

The authors have no conflicts to disclose.

Author Contributions

Masafumi Horio: Data curation (lead); Formal analysis (lead); Writing – original draft (equal); Writing – review & editing (equal). **Yuya Kubota:** Data curation (supporting); Resources (equal). **Shigeki Owada:** Resources (equal). **Kensuke Tono:** Resources (equal). **Makina Yabashi:** Resources (lead). **Takushi Iimori:** Data curation (supporting). **Yoshihiro Miyauchi:** Methodology (supporting). **Michael Zuerch:** Conceptualization (equal); Funding acquisition (equal); Methodology (supporting); Project administration (equal); Supervision (equal); Writing – review & editing (supporting). **Iwao Matsuda:** Data curation (supporting); Project administration (equal); Resources (equal); Supervision (equal); Writing – original draft (lead). **Craig Philip Schwartz:** Conceptualization (equal); Data curation (supporting); Funding acquisition (equal); Project administration (equal); Supervision (equal); Writing – review & editing (supporting). **Walter Drisdell:** Conceptualization (lead); Data curation (supporting); Funding acquisition (lead); Project administration (lead); Supervision (equal); Writing – review & editing (equal). **Toshihide Sumi:** Data curation (equal); Funding acquisition (supporting). **James Bullock:** Conceptualization (supporting); Data curation (equal); Funding acquisition (equal). **Yasuyuki Hirata:** Data curation (supporting); Methodology (supporting). **Masashige Miyamoto:** Data curation (equal); Formal analysis (supporting). **Bailey R. Nebgen:** Data curation (supporting); Formal analysis (supporting); Writing – review & editing (supporting). **Tetsuya Wada:** Data curation (supporting). **Tomoaki Senoo:** Data curation (supporting). **Yuki Tsujikawa:** Data curation (supporting).

DATA AVAILABILITY

The data that support the findings of this study are available from the corresponding author upon reasonable request.

REFERENCES

[1]X. Yang, Q. Bi, H. Ali, K. Davis, W. V. Schoenfeld, and K. Weber, Adv. Mater. **28**, 5891–5897 (2016).
[2]T. Matsui, M. Bivour, P. F. Ndione, R. S. Bonilla, and M. Hermle, Sol. Energy Mater. Sol. Cells **209**, 110461 (2020).
[3]T. Matsui, S. McNab, R. S. Bonilla, and H. Sai, ACS Appl. Energy Mater. **5**, 12782–12789 (2022).

[4]G. Dingemans and W. M. M. Kessels, J. Vac. Sci. Technol. A **30**, 040802 (2012).
[5]J. Bullock, P. Zheng, Q. Jeangros, M. Tosun, M. Hettick, C. M. Sutter-Fella, Y. Wan, T. Allen, D. Yan, D. Macdonald, S. De Wolf, A. Hessler-Wyser, A. Cuevas, and A. Javey, Adv. Energy Mater. **6**, 1600241 (2016).
[6]J. Bullock, Y. Wan, M. Hettick, X. Zhaoran, S. P. Phang, D. Yan, H. Wang, W. Ji, C. Samundsett, Z. Hameiri, D. Macdonald, A. Cuevas, and A. Javey, Adv. Energy Mater. **9**, 1803367 (2019).
[7]T. G. Allen, J. Bullock, Q. Jeangros, C. Samundsett, Y. Wan, J. Cui, A. Hessler-Wyser, S. De Wolf, A. Javey, and A. Cuevas, Adv. Energy Mater. **7**, 1602606 (2017).
[8]I. Matsuda and Y. Kubota, Chem. Lett. **50**, 1336 (2021).
[9]S. Yamamoto, T. Omi, H. Akai, Y. Kubota, Y. Takahashi, Y. Suzuki, Y. Hirata, K. Yamamoto, R. Yukawa, K. Horiba, H. Yumoto, T. Koyama, H. Ohashi, S. Owada, K. Tono, M. Yabashi, E. Shigemasa, S. Yamamoto, M. Kotsugi, H. Wadati, H. Kumigashira, T. Arima, S. Shin, and I. Matsuda, Phys. Rev. Lett. **120**, 223902 (2018).
[10]R. K. Lam, S. L. Raj, T. A. Pascal, C. D. Pemmaraju, L. Foglia, A. Simoncig, N. Fabris, P. Miotti, C. J. Hull, A. M. Rizzuto, J. W. Smith, R. Mincigrucci, C. Masciovecchio, A. Gessini, E. Allaria, G. De Ninno, B. Diviacco, E. Roussel, S. Spampinati, G. Penco, S. Di Mitri, M. Trovò, M. Danailov, S. T. Christensen, D. Sokaras, T.-C. Weng, M. Coreno, L. Poletto, W. S. Drisdell, D. Prendergast, L. Giannessi, E. Principi, D. Nordlund, R. J. Saykally, and C. P. Schwartz, Phys. Rev. Lett. **120**, 023901 (2018).
[11]E. Berger, S. Jamnuch, C. B. Uzundal, C. Woodahl, H. Padmanabhan, A. Amado, P. Manset, Y. Hirata, Y. Kubota, S. Owada, K. Tono, M. Yabashi, C. Wang, Y. Shi, V. Gopalan, C. P. Schwartz, W. S. Drisdell, I. Matsuda, J. W. Freeland, T. A. Pascal, and M. Zuerch, Nano Lett. **21**, 6095 (2021).
[12]C. B. Uzundal, S. Jamnuch, E. Berger, C. Woodahl, P. Manset, Y. Hirata, T. Sumi, A. Amado, H. Akai, Y. Kubota, S. Owada, K. Tono, M. Yabashi, J. W. Freeland, C. P. Schwartz, W. S. Drisdell, I. Matsuda, T. A. Pascal, A. Zong, and M. Zuerch, Phys. Rev. Lett. **127**, 237402 (2021).
[13]C. P. Schwartz, S. L. Raj, S. Jamnuch, C. J. Hull, P. Miotti, R. K. Lam, D. Nordlund, C. B. Uzundal, C. Das Pemmaraju, R. Mincigrucci, L. Foglia, A. Simoncig, M. Coreno, C. Masciovechio, L. Giannessi, L. Poletto, E. Principi, M. Zuerch, T. A. Pascal, W. S. Drisdell, and R. J. Saykally, Phys. Rev. Lett. **127**, 096801 (2021).
[14]A. Zong, B. R. Nebgen, S.-C. Lin, J. A. Spies, and M. Zuerch, Nat. Rev. Mater. **8**, 224 (2023).
[15]C. Woodahl, S. Jamnuch, A. Amado, C. B. Uzundal, E. Berger, P. Manset, Y. Zhu, Y. Li, D. D. Fong, J. G. Connell, Y. Hirata, Y. Kubota, S. Owada, K. Tono, M. Yabashi, S. Tepavcevic, I. Matsuda, W. S. Drisdell, C. P. Schwartz, J. W. Freeland, T. A. Pascal, A. Zong, and M. Zuerch, Nat. Mater. **22**, 848–852 (2023).
[16]T. Ishikawa, H. Aoyagi, T. Asaka, Y. Asano, N. Azumi, T. Bizen, H. Ego, K. Fukami, T. Fukui, Y. Furukawa, S. Goto, H. Hanaki, T. Hara, T. Hasegawa, T. Hatsui, A. Higashiya, T. Hirono, N. Hosoda, M. Ishii, T. Inagaki, Y. Inubushi, T. Itoga, Y. Joti, M. Kago, T. Kameshima, H. Kimura, Y. Kirihara, A. Kiyomichi, T. Kobayashi, C. Kondo, T. Kudo, H. Maesaka, X. M. Maréchal, T. Masuda, S. Matsubara, T. Matsumoto, T. Matsushita, S. Matsui, M. Nagasono, N. Nariyama, H. Ohashi, T. Ohata, T. Ohshima, S. Ono, Y. Otake, C. Saji, T. Sakurai, T. Sato, K. Sawada, T. Seike, K. Shirasawa, T. Sugimoto, S. Suzuki, S. Takahashi, H. Takebe, K. Takeshita, K. Tamasaku, H. Tanaka, R. Tanaka, T. Tanaka, T. Togashi, K. Togawa, A. Tokuhisa, H. Tomizawa, K. Tono, S. Wu, M. Yabashi, M. Yamaga, A. Yamashita, K. Yanagida, C. Zhang, T. Shintake, H. Kitamura, and N. Kumagai, Nat. Photonics **6**, 540 (2012).
[17]S. Owada, K. Togawa, T. Inagaki, T. Hara, T. Tanaka, Y. Joti, T. Koyama, K. Nakajima, H. Ohashi, Y. Senba, T. Togashi, K. Tono, M. Yamaga, H. Yumoto, M. Yabashi, H. Tanaka, and T. Ishikawa, J. Synchrotron Radiat. **25**, 282 (2018).
[18]Y. Kubota, H. Motoyama, G. Yamaguchi, S. Egawa, Y. Takeo, M. Mizuguchi, H. Sharma, S. Owada, K. Tono, H. Mimura, I. Matsuda, and M. Yabashi, Appl. Phys. Lett. **117**, 042405 (2020).
[19]T. Kimura, Y. Takeo, K. Sakurai, N. Furuya, S. Egawa, G. Yamaguchi, Y. Matsuzawa, T. Kume, H. Mimura, M. Shimura, H. Ohashi, I. Matsuda, and Y. Harada, Opt. Express **30**, 26220 (2022).
[20]T. Sumi, M. Horio, T. Senoo, T. Wada, Y. Tsujikawa, X. Zhang, P. Manset, M. Araki, Y. Hirata, W. S. Drisdell, J. W. Freeland, A. Amado, M. Zuerch, Y. Kubota, S. Owada, K. Tono, M. Yabashi, C. P. Schwartz, and I. Matsuda, Surf. Sci. Nanotechnol. **20**, 31 (2022).
[21]T. Sumi, T. Senoo, M. Horio, S. El Moussaoui, E. Nakamura, K. Tanaka, A. Tsukamoto, and I. Matsuda, Jpn. J. Appl. Phys. **62**, SB8001 (2023).
[22]M. Araki, J. Meikaku, Y. Kubota, J. Miyawaki, Y. Kosegawa, S. El Moussaoui, T. Bouillaud, P. Manset, S. Owada, K. Tono, M. Yabashi, and I. Matsuda, Surf. Sci. Nanotechnol. **18**, 231 (2020).
[23]X. Wang, K. Han, W. Wang, J. Xiang, H. Yang, J. Zhang, X. Ma, C. Zhao, D. Chen, and T. Ye, Appl. Phys. Lett. **100**, 122907 (2012).
[24]F. J. Himpsel, F. R. McFeely, A. Taleb-Ibrahimi, A. J. A. Yarmoff, and G. Hollinger, Phys. Rev. B **38**, 6084 (1988).
[25]J. Bullock, M. Hettick, J. Geissbühler, A. J. Ong, T. Allen, C. M. Sutter-Fella, T. Chen, H. Ota, E. W. Schaler, S. De Wolf, C. Ballif, A. Cuevas, and A. Javey, Nat. Energy **1**, 15031 (2016).
[26]S. E. Shaheen, G. E. Jabbour, M. M. Morrell, Y. Kawabe, B. Kippelen, N. Peyghambarian, M.-F. Nabor, R. Schlaf, E. A. Mash, and N. R. Armstrong, J. Appl. Phys. **84**, 2324 (1998).
[27]R. Yukawa, S. Yamamoto, K. Ozawa, M. Emori, M. Ogawa, S. Yamamoto, K. Fujikawa, R. Hobara, S. Kitagawa, H. Daimon, H. Sakama, and I. Matsuda, Appl. Phys. Lett. **105**, 151602 (2014).
[28]M. Ogawa, S. Yamamoto, K. Fujikawa, R. Hobara, R. Yukawa, S. Yamamoto, S. Kitagawa, D. Pierucci, M. G. Silly, C.-H. Lin, R.-Y. Liu, H. Daimon, F. Sirotti, S.-J. Tang, and I. Matsuda, Phys. Rev. B **88**, 165313 (2013).
[29]M. D'Angelo, R. Yukawa, K. Ozawa, S. Yamamoto, T. Hirahara, S. Hasegawa, M. G. Silly, F. Sirotti, and I. Matsuda, Phys. Rev. Lett. **108**, 116802 (2012).
[30]K. Ozawa, M. Emori, S. Yamamoto, R. Yukawa, S. Yamamoto, R. Hobara, K. Fujikawa, H. Sakama, and I. Matsuda, J. Phys. Chem. Lett. **5**, 1953–1957 (2014).
[31]R. Yukawa, S. Yamamoto, K. Akikubo, K. Takeuchi, K. Ozawa, H. Kumigashira, and I. Matsuda, Adv. Mat. Interfaces **3**, 1600527 (2016).